Long-term effects of waste brick powder addition in the microstructure and service properties of mortars

José Marcos Ortega[1], Viviana Letelier[2], Carlos Solas[1], Giacomo Moriconi[3], Miguel Ángel Climent[1] and Isidro Sánchez [1,*]

[1] Departamento de Ingeniería Civil, Universidad de Alicante, Ap. Correos 99, 03080, Alacant/Alicante, Spain;

[2] Departamento de Obras Civiles, Universidad de la Frontera, Av. Fco. Salazar 01145, Temuco, Chile.

[3] Department of Science and Engineering of Matter, Environment and Urban Planning, Università Politecnica delle Marche,Via Brecce Bianche, 60131, Ancona, Italy.

* Correspondence: isidro.sanchez@ua.es; Tel.: +34-96-5903-400 (ext. 2090)

Con formato: Español (alfab. internacional)

Abstract: One way to reach a more sustainable cement industry is replacing clinker by additions, such as waste brick powder. The objective of this research is to analyse the influence in the long-term (until 400 days) of waste brick powder in the microstructure, durability and mechanical properties of mortars which incorporate up to 20% of this addition as a clinker replacement. The microstructure has been studied with the non-destructive impedance spectroscopy technique. According to the obtained results, mortars with 10% and 20% of brick powder, showed good service properties in the long-term, even better than those made with ordinary Portland cement.

Keywords: waste brick powder; sustainability; microstructure; impedance spectroscopy; durability; mechanical properties.

1. Introduction

Nowadays, one of the industrial sectors which more pollution produces worldwide is the cement manufacture. Therefore, reaching a more environmentally sustainable cement industry still constitutes an important challenge, especially in search of reducing the CO_2 emissions generated

along the cement production. One of the most common ways to lessen those emissions is replacing partially, or even totally, clinker by supplementary cementitious materials or other additions in general [1–3][1–3] . Ground granulated blast-furnace slag, fly ash and silica fume are now some of the most popular additions [4–7] [4–6] , and cements including those additions are produced at industrial scale. Furthermore, many additions, such as the abovementioned ones, are pollutant wastes produced during other industrial processes, so their reuse would partly solve other environmental problems, like their storage.

For those reasons, the research about new suitable cement additions is still the topic of many studies [7,8]. Among those additions, the study of brick powder as clinker replacement has been the topic of recent researches [9–12]. In the abovementioned studies, the effects of brick powder in cement-based materials properties have overall been studied in the short-term (up to 120 hardening days), and this addition came from construction and demolition wastes, as well as from defective bricks rejected along the manufacturing works.

Regarding this addition, several studies [9,11,13–16] have determined that brick powder is a pozzolanic material. Its pozzolanic activity is produced as a consequence of the transformation of crystalline structures of clay silicates in amorphous compounds along the manufacture process of bricks [17], in which clay is exposed to high temperatures, ranging from 600ºC to 1000ºC. Other researches about the use of brick powder in mortars and concretes [10,18–20] have pointed out that a cement replacement up to a 20% of brick powder could be suitable, and it would not affect the physical and mechanical properties of the material. Moreover, it has been noted that the particle size is an important factor in order to insure an adequate behaviour of this addition [21], and it has also been pointed out that the best mechanical strength performance is obtained when the particle size of brick powder is less than 0.06 mm [22].

In addition to this, Schackow et al. [12] have concluded that the reaction between the amorphous compounds of brick powder, such as silica and alumina, with calcium hydroxide generates silicate/aluminate hydrates similar to those produced in the cement hydration.

Furthermore, according to the abovementioned work of Schackow et al. [12], another factor that could have an influence in the good performance of cement binders with brick powder, would be the filler effect of this addition, because it would occupy the pre-existing voids present in the pore network of the materials, reducing in this way their pore sizes.

On the other hand, the study of the microstructure of cement-based materials is important, because it is related to their mechanical and durability-related properties [23]. Among the different techniques for characterising the microstructure, the novel non-destructive impedance spectroscopy has recently experienced a great development, becoming popular for the study of different cement-based materials, such as those prepared using slag and fly ash cements [24,25][24,25], as well as exposed to aggressive [26,27][26,27] or non-optimum environments [28–30][28]. Nevertheless, the impedance spectroscopy technique has never been used for studying the evolution of the microstructure of cement mortars which incorporate waste brick powder.

Other uses of this waste have been as aggregate in hydraulic lime mortars [29] or colouring additive for plaster [30], with no structural intention.

Therefore, the main objective of this research is to study the influence in the long-term (until 400 days) of the addition of waste brick powder in the microstructure, durability and mechanical properties of mortars which incorporate up to 20% of this addition as a clinker replacement. As a reference, mortars made using ordinary Portland cement without additions were also studied. The non-destructive impedance spectroscopy technique and mercury intrusion porosimetry (as contrast technique) were used in order to characterise the microstructure of the specimens, and its time evolution. Moreover, differential thermal analysis of the mortars was also performed, in order to check the pozzolanic activity of the waste. Durability-related parameters, the effective porosity, the capillary suction coefficient, the steady-state diffusion coefficient obtained from saturated sample's resistivity and the non-steady state chloride migration coefficient were analysed, to ensure that the addition of the brick powder will not worsen these properties. Finally, for checking the mechanical behaviour of the mortars, their flexural and compressive strengths were also obtained.

2. Materials and Methods

2.1. Waste brick powder characterisation

Waste brick powder was obtained from industrial brick residuals from demolition debris. Particles under 75 μm were selected after grinding and sieving the brick powder. The results of the chemical and physical analysis are shown in Table 1.

Blaine values specified in Table 1 were obtained following the ASTM C204 specifications [31]. The values show that bricks powder presented higher specific surface than cement, agreeing with previous studies [9].

The mineralogical study of the brick powder on dry powder was carried out using XRD. The inorganic crystalline phases identified in the XRD patterns (Figure 1Figure 1) were silica (sand used to adjust the plasticity of the brick green mixture), illite (main mineralogical constituent of the clay used in brick manufacture), and hematite (used to reduce the firing temperature and favour the formation of liquid phases).

Con formato: Inglés (Reino Unido)

Table 1. Physical and chemical properties of waste brick powder

Composition	Brick powder
SiO_2	41.47 %
Al_2O_3	39.05 %
CaO	0.63 %
Fe_2O_3	12.73 %
SO_3	1.59 %
MgO	-
Na_2O	-
K_2O	2.81 %
TiO_2	1.03 %
CuO	0.70 %
Density	2660 kg/m^3
Blaine surface area	6485 m^2/kg

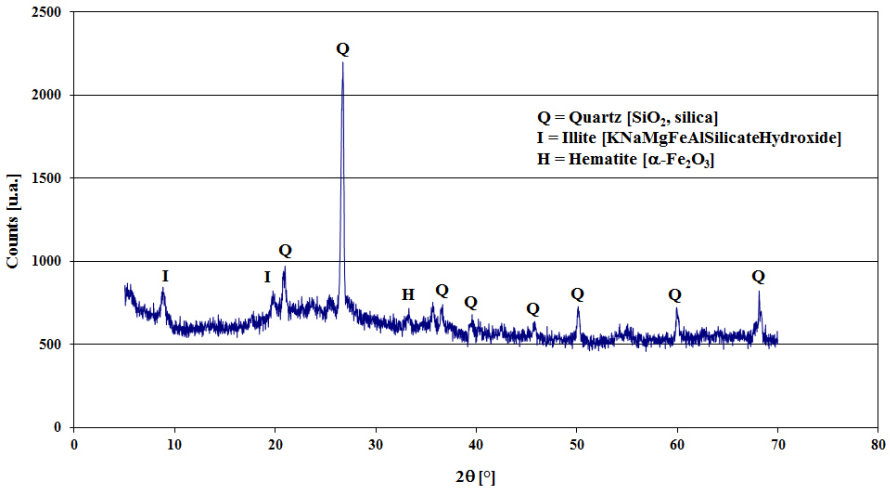

Figure 1. XRD pattern of brick powder.

In Figure 2Figure 2 SEM observation is reported, showing that waste brick powder consisted of morphologically irregular particles, whilst the elemental analysis (see Figure 3Figure 3) was substantially consistent with the XRD analysis. Finally, the particle size distribution of the waste brick powder used is shown in Figure 4Figure 4.

Con formato: Inglés (Reino Unido)

Con formato: Inglés (Reino Unido)

Con formato: Inglés (Reino Unido)

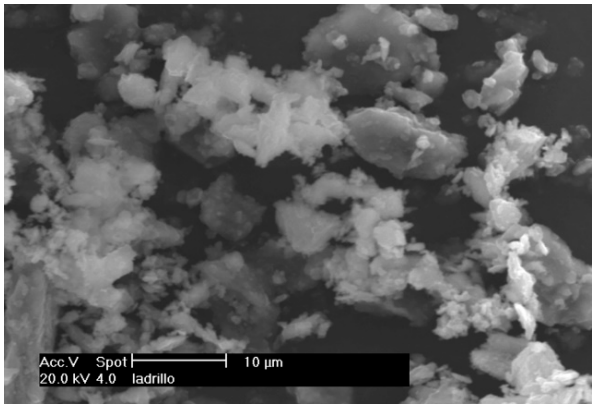

Figure 2. (a) SEM micrograph of brick powder.

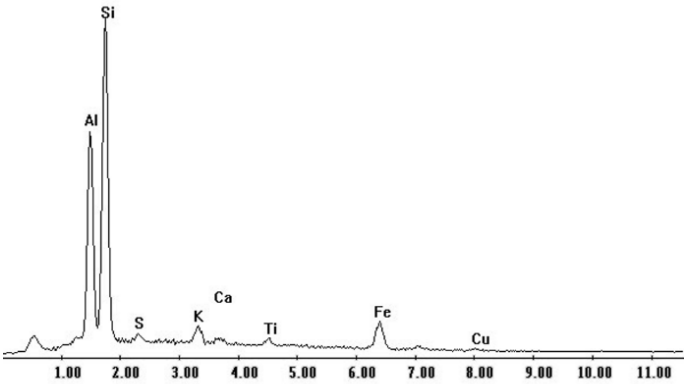

Figure 3. EDS analysis of brick powder.

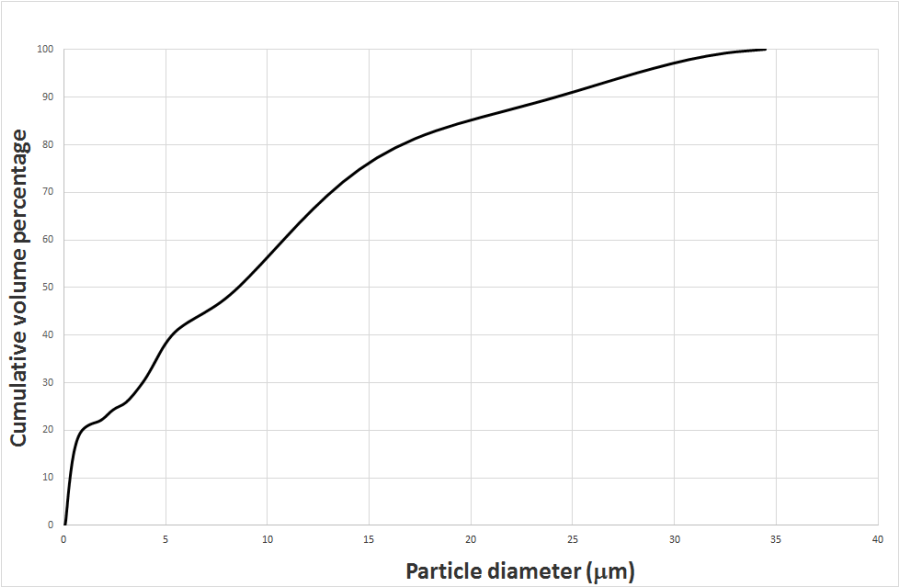

Figure 4. Particle size distribution of waste brick powder.

2.2. Sample preparation

Three types of cement mortars were studied in this work. The first one was prepared using a commercial ordinary Portland cement, designated CEM I 42.5 R (CEM I hereafter), according to the Spanish and European standard UNE-EN 197-1 [32]. Moreover, two blended cements, which incorporate waste brick powder, were used. Both blended cements were made with an ordinary Portland cement, CEM I 42.5 R [32], which was replaced by 10% and 20% of brick powder. They will be referred as BP10 and BP20 respectively from now on. The water to cement ratio was 0.5 for all the

mortars, and the aggregate to cement ratio was 3:1. Aggregates used were siliceous, with the granulometry according the the prescriptions of the standard UNE-EN 196-1

Two kinds of specimens were prepared. The first type consisted of cylindrical specimens of 10 cm diameter and 15 cm height, and the second one consisted of prismatic samples with dimensions 4 cm x 4 cm x 16 cm [33]. Both kinds of samples were maintained in 95% relative humidity (RH) chamber and 20ºC for the first 24 hours. After that, they were de-moulded and the 10 cm-diameter and 15 cm-height cylindrical samples were cut to obtain different cylinders of 1 cm and 5 cm thickness. Finally, all the samples were kept under an optimum laboratory condition (20ºC and 100% RH) until the testing ages.

2.3. Mercury intrusion porosimetry

The classical mercury intrusion was used in order to study the microstructure of the mortars, in spite of its drawbacks [34,35]. The tests were performed with a porosimeter model Poremaster-60 GT from Quantachrome Instruments. Before the test, samples were oven dried for 48 hours at 50ºC. Total porosity, pore size distribution and percentage of Hg retained at the end of the experiment were studied. The testing ages were 28, 100, 200 and 400 days.

2.4. Impedance spectroscopy

The evolution of the pore structure of the mortars has also been studied using the non-destructive impedance spectroscopy technique. This technique has several advantages in comparison with other classical ones, because it allows obtaining global information of the specimens pore network [36,37][36,37], as well as to study the microstructure changes of the same sample during the studied period [38,39][28]. In recent years, several works [27,39][38,39] have been published in which this technique has been used for following the evolution of the pore structure of cement-based materials which incorporate well-known additions. However, there is no experience

about using impedance spectroscopy for studying cement-based materials which incorporates brick powder as clinker replacement.

The impedance spectroscopy measurements were performed using an Agilent 4294A analyser. This analyser permits capacitance measurements in the range from 10^{-14} F to 0.1 F, with a maximum resolution of 10^{-15} F. In this work, the frequencies for obtaining the impedance spectra ranged between 100 Hz and 100 MHz. The electrodes used for performing the measurements were circular (Ø = 8 cm) and made of flexible graphite, attached to a copper piece with the same diameter. Both contacting and non-contacting methods were used [40]. An example of the measurement using each experimental setup is shown in Figure 5Figure 5.

Samples were in a close to saturation state since they were stored under 100% RH, fact that ensures absence of drying on samples, so it was not necessary to saturate them before measuring the impedance spectra.

The measurements were validated using the Kramers–Kronig (K–K) relations [41] (see Figure 6.a) and the differential impedance analysis [42] was applied to them (see Figure 6Figure 6.b). As it can be seen, the measurement is valid and it contains two time constants in the measured spectra, with independence of the experimental setup. This result permits to fit the experimental data to the equivalent circuits proposed by Cabeza et al. [40] (see Figure 5), which include two time constants. Those circuits are constituted by several resistances and capacitances, which are related to different elements of the microstructure of cement-based materials [37]. On one hand, the resistance R_1 is associated only with the percolating pores of the sample, while the resistance R_2 provides information about all its pores. On the other hand, the capacitance C_1 is related to the solid fraction of the sample and the capacitance C_2 is associated to the pore surface in contact with the electrolyte which fills the pore network of the material [37].As can be observed in Figure 5Figure 5, the impedance parameters R_2, C_1 and C_2 are present in both contacting and non-contacting methods. In this research, only the values of these parameters (R_2, C_1 and C_2) obtained with non-contacting method have been studied, due to its higher accuracy. The value of the resistance R_1 can only be

Con formato: Inglés (Reino Unido)

Con formato: Inglés (Reino Unido)
Con formato: Fuente: Cursiva
Con formato: Fuente: Cursiva
Con formato: Fuente: Cursiva
Con formato: Fuente: Cursiva
Con formato: Fuente: Cursiva
Con formato: Fuente: Cursiva
Con formato: Fuente: Cursiva
Con formato: Fuente: Cursiva
Con formato: Fuente: Cursiva
Con formato: Fuente: Cursiva
Con formato: Inglés (Reino Unido)
Con formato: Fuente: Cursiva
Con formato: Fuente: Cursiva
Con formato: Fuente: Cursiva
Con formato: Fuente: Cursiva
Con formato: Fuente: Cursiva
Con formato: Fuente: Cursiva
Con formato: Fuente: Cursiva
Con formato: Fuente: Cursiva
Con formato: Fuente: Cursiva
Con formato: Fuente: Cursiva
Con formato: Fuente: Cursiva
Con formato: Sin Superíndice / Subíndice
Con formato: Fuente: Cursiva
Con formato: Fuente: Cursiva, Subíndice

obtained by using the contacting method, and the values of this resistance have been obtained from the contacting measurements.

Eight different disks of approximately 1 cm thickness were tested for each cement type. The evolution of impedance parameters with time has been reported to over a 400 hardening days.

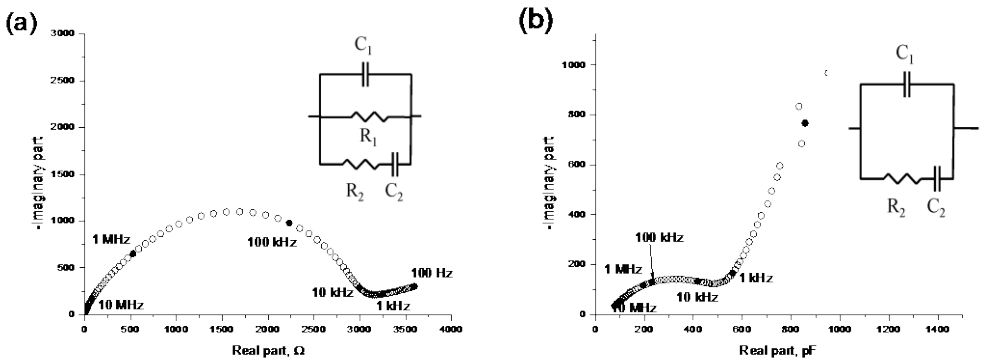

Figure 5. (a) Nyquist plot obtained for a BP20 mortar at 20 hardening days and the equivalent circuit used for the fitting of the impedance spectra obtained using the contacting method. (b) Cole-Cole plot for a BP20 mortar at 37 hardening days and the equivalent used for the fitting of the impedance spectra obtained using the non-contacting method.

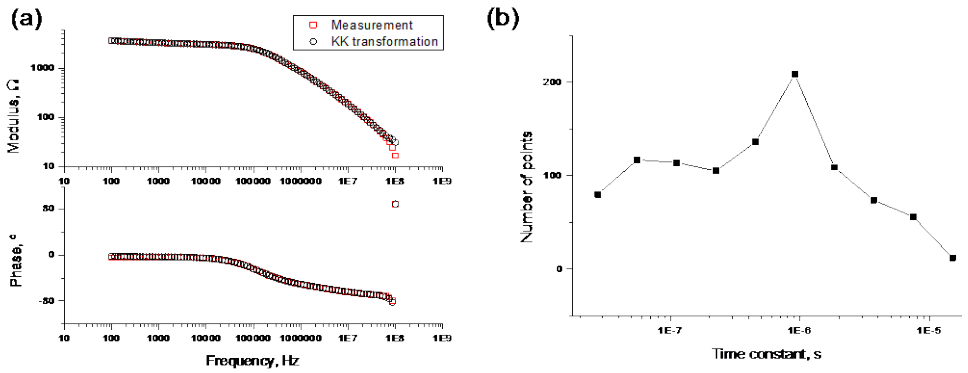

Figure 6. (a) Bode plot obtained at 20 hardening days for the BP20 mortar of Figure 5Figure 5.a validated using the Kramers-Kronig (K-K) relations (see the text for details). (b) Differential impedance analysis of

Con formato: Fuente: 9 pto

the impedance spectrum shown in Figure 6Figure 6.a. The two maxima in the plot reveal the presence of two time constants in the impedance spectrum.

Con formato: Fuente: 9 pto

2.5. Differential Thermal Analysis

The differential thermal analysis was performed using a simultaneous TG-DTA model TGA/SDTA851e/SF/1100 from Mettler Toledo, capable of working between room temperature and 1100ºC. The selected heating ramp was 20ºC/min up to 1000ºC in N_2 atmosphere. The curves weigh derivate versus temperature were studied for each mortar type at 15 and 90 days.

2.6. Capillary absorption test

The capillary absorption test was performed according to the standard UNE 83982 [43], which is based on the Fagerlund method to determine the capillarity of concrete. In relation to the pre-conditioning procedure, firstly the samples were completely dried in an oven at 105ºC for 12 h and, since then until the beginning of the test they were kept in a hermetically sealed container with silica gel during the next 12 h [45–47][44]. Furthermore, prior to the test, the circumferential surface of the specimens was sealed using self-adhesive tape [46,47][45].

The test was performed using a container with a flat base, in which the samples were placed according to the UNE 83982 [43]. Along the test, the level of distilled water was kept constant at 5±1 mm on the lateral surface of the specimens. In addition to this, the abovementioned standard [43] establishes that more than a 95% of the base of the sample should be in contact with water. The container was hermetically closed throughout the test. Samples were weighed at different times set in the standard [43]. The test finished when the difference between two consecutive weights was lower than 0.1%, in mass, with 24 hours difference. Finally, the capillary suction coefficient and effective porosity were calculated according to the expressions:

$$\varepsilon_e = \frac{Q_n - Q_0}{A \cdot h \cdot \delta_a} \quad (1)$$

$$K = \frac{\delta_a \cdot \varepsilon_e}{10 \cdot \sqrt{m}} \text{ with } m = \frac{t_n}{h^2} \quad (2)$$

Where: ε_e is the effective porosity. Q_n is the weight of the sample at the end of the test (g). Q_0 is the weight of the sample before starting the test (g). A is the surface of the sample in contact with water (cm^2). h is the thickness of the sample (cm). δ_a is the density of water (1 g/cm^3). K is the capillary suction coefficient ($kg/m^2min^{0.5}$). m is the resistance to water penetration by capillary suction (min/cm^2). t_n is the time necessary to reach the saturation (minutes).

For each cement type, three different cylinders of 10 cm diameter and 5 cm thickness were tested at 28, 200 and 400 days.

2.7. Steady-state diffusion coefficient obtained from saturated sample's resistivity

The electrical resistivity gives information about the pores connectivity of cement-based materials, as well as permits to determine their steady-state chloride diffusion coefficient (D_S) [46]. Here, the resistivity was calculated from the impedance spectroscopy R_1 values obtained in saturated cylindrical specimens of 10 cm diameter and 5 cm thickness. As has been explained in the section 2.4, the impedance resistance R_1 is associated to pores which cross the sample [40], and therefore it is equivalent to the electrical resistance of sample [48,49][44]. The studied samples were saturated for 24 h according to ASTM Standard C1202 [31][48] and they were used later for the forced migration tests. The steady-state ionic diffusion coefficient was calculated according to the expression [46]:

$$D_S = \frac{2 \cdot 10^{-10}}{\rho} \quad (3)$$

Where: D_s is the chloride steady-state diffusion coefficient through the sample (m^2/s). ρ is the electrical resistivity of specimen ($\Omega \cdot m$).

For each cement type, three different samples were tested at 28, 200 and 400 days.

Con formato: Fuente: Cursiva

237

238 *2.8. Forced migration test*

239 The forced chloride migration test was performed on water-saturated mortar samples,
240 according to NT Build 492 [47]. The main result of this test is the non-steady-state chloride migration
241 coefficient D_{NTB}. For each cement type, three different cylindrical samples of 10 cm diameter and 5
242 cm height were tested at 28, 200 and 400 hardening ages.

243

244 *2.9. Mechanical strength test*

245 The compressive and flexural strengths were determined according to the standard UNE-EN
246 196-1 [33]. Three different prismatic samples with dimensions 4 cm x 4 cm x 16 cm were tested for
247 each cement type at 28, 200 and 400 hardening ages.

248

249 **3. Results**

250 *3.1. Mercury intrusion porosimetry*

251 The results of total porosity for CEM I, BP10 and BP20 mortars are depicted in Figure 7Figure 7.
252 This parameter decreased from 28 to 200 days for all the studied mortars, mainly between 28 and 100
253 days, and since 200 days it kept practically constant or slightly increased depending on the content
254 of addition. In general, the total porosity was higher for BP20 mortars up to 200 days, and it was very
255 similar for both CEM I and BP10 ones. However, there were hardly differences in total porosity at
256 400 days for the three types of analysed mortars.

257 The pore size distributions for the studied specimens are shown in Figure 8Figure 8. The
258 microstructure was more refined for mortars with brick powder, as indicated their higher relative
259 volume of pores of the ranges <10 nm and 10-100 nm. Moreover, this pore refinement was greater as
260 the percentage of addition was higher. For CEM I specimens, the pore size distribution hardly
261 changed with age. On the other hand, for BP10 and BP20 mortars, the microstructure became more
262 refined with time, as showed the progressive increase of percentage of finer pores.

Con formato: Inglés (Reino Unido)

Con formato: Inglés (Reino Unido)

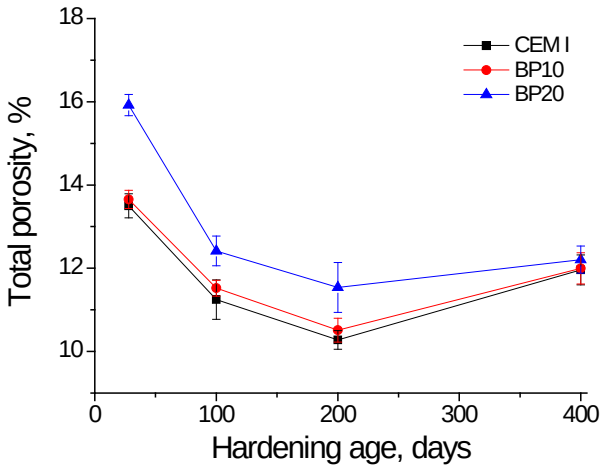

Figure 7. Results of total porosity for mortars prepared using only ordinary Portland cement (CEM I), and for those with a content of 10% (BP10) and 20% (BP20) of brick powder.

The results of percentage of Hg retained in the samples at the end of the experiment are depicted in Figure 9. Along the studied period, the highest values of this parameter corresponded to brick powder mortars. Until 200 days, the Hg retained generally increased for all the specimens, and since then up to 400 days it kept practically constant or slightly decreased depending on the mortar typedecreased for the mortar with no addition of brick powder, and increased for the mortar with a 10% of addition of the waste. For samples with 20% of addition there was a decrease in the retained mercury, but lower than for the OPC.

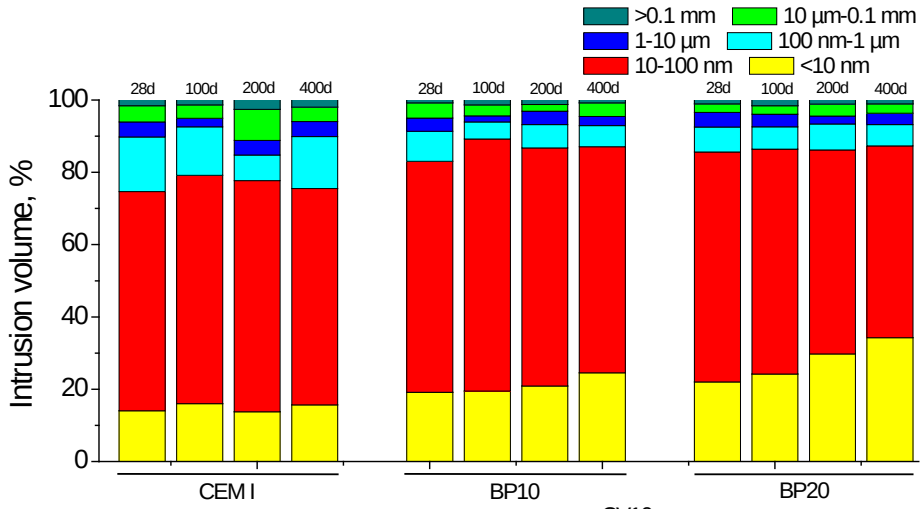

Figure 8. Pore size distributions obtained for the three types of studied mortars.

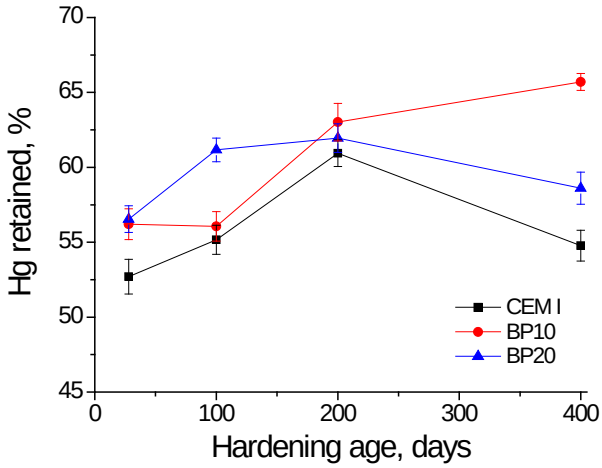

Figure 9. Results of mercury retained at the end of mercury intrusion porosimetry test for the studied mortars.

3.2. Impedance spectroscopy

The results of resistance R_1 can be observed in Figure 10. In general, this parameter rose with age for the three types of mortars studied. Nevertheless, the increasing rate of the resistance R_1 was higher for specimens with brick powder, and as a consequence, the values of this parameter were greater for those specimens compared to CEM I ones, especially from 100 hardening days. The values of resistance R_1 were very similar for both BP10 and BP20 mortars over the studied time

Con formato: Fuente: Cursiva
Con formato: Fuente: Cursiva
Con formato: Fuente: Cursiva
Con formato: Fuente: Cursiva
Con formato: Fuente: Cursiva
Con formato: Fuente: Cursiva

period. As it can be seen in the enlarged area of Figure 10, the initial values of resistance are higher for mortars prepared with brick powder, and greater for BP20.

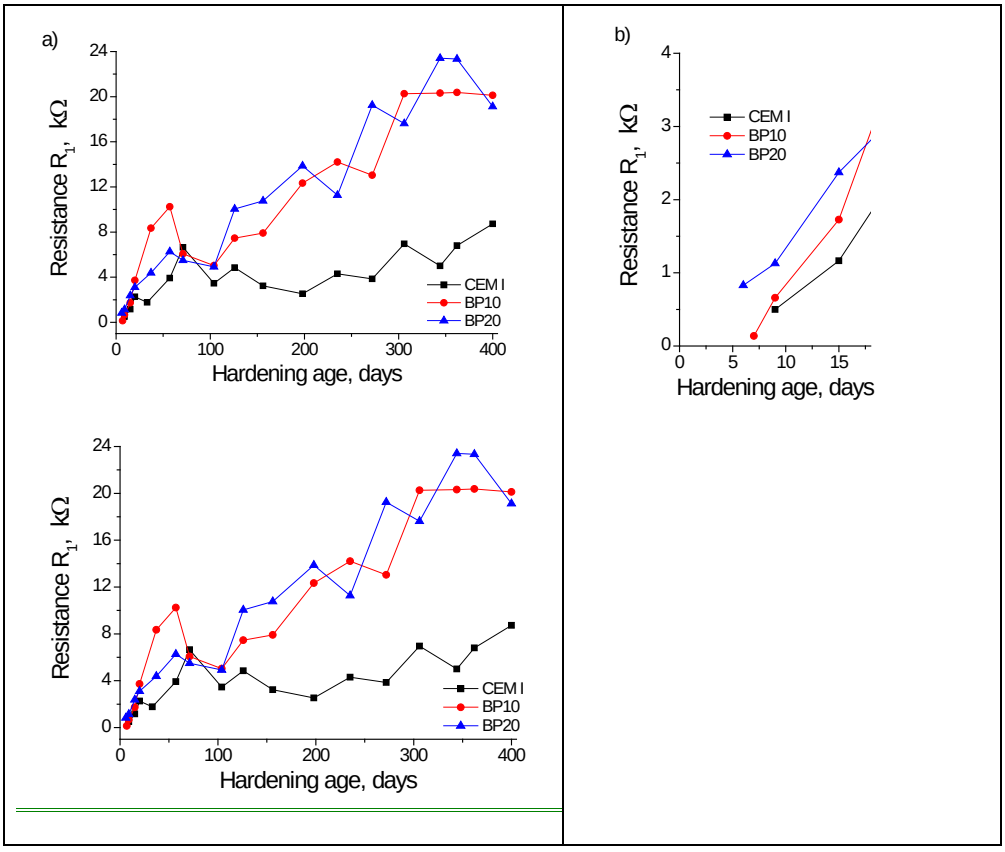

Figure 10. a) Results of impedance spectroscopy resistance R_1 for the studied mortars. b) Zoomed area of the initial behaviour of the resistance.

Tabla con formato

Con formato: Fuente: Cursiva

Con formato: Fuente: Cursiva

With respect to resistance R_2, its results are shown in Figure 11. This parameter rose with hardening age for mortars which incorporated brick powder and hardly changed for CEM I samples. The resistance R_2 increasing rate was higher for BP20 mortars in comparison with BP10 ones. At 400 days, the greatest values of this parameter were noted for BP20 specimens and the lowest R_2 were observed for CEM I mortars. Moreover, equivalent behaviour as R_1 has been found in the initial days.

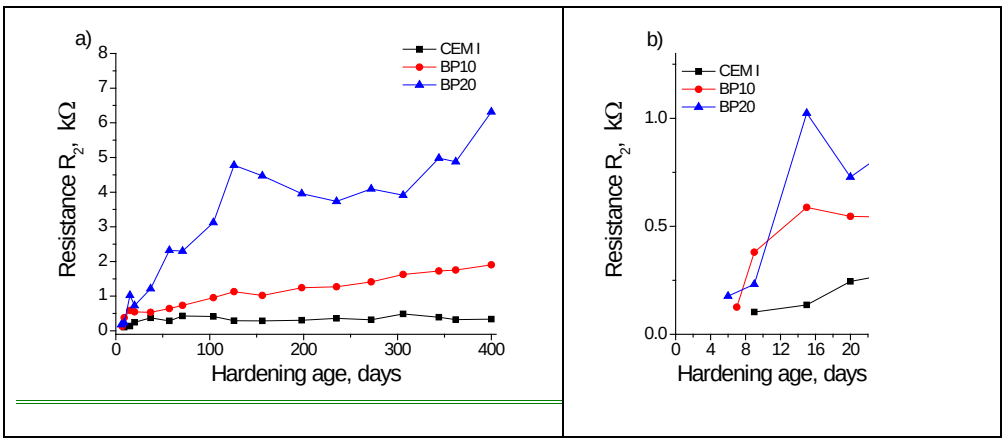

Figure 11. a) Results of impedance spectroscopy resistance R_2 for the studied mortars.b) Zoomed area of the initial behaviour of the resistance

The evolution of capacitance C_1 is shown in Figure 12Figure 12. This parameter was overall similar for the three kinds of analysed mortars. It grew relatively faster at early ages, but since 100 days approximately it kept practically constant. The capacitance C_1 values were slightly higher for mortars with brick powder, even though they showed the higher porosity.

Con formato: Fuente: Cursiva
Con formato: Fuente: Cursiva
Con formato: Fuente: Cursiva
Con formato: Fuente: Cursiva
Con formato: Fuente: Cursiva
Con formato: Fuente: Cursiva
Con formato: Fuente: Cursiva
Con formato: Fuente: Cursiva
Con formato: Fuente: Cursiva
Tabla con formato
Con formato: Fuente: Cursiva
Con formato: Fuente: Cursiva
Con formato: Fuente: Cursiva
Con formato: Fuente: Cursiva
Con formato: Inglés (Reino Unido)
Con formato: Fuente: Cursiva
Con formato: Fuente: Cursiva

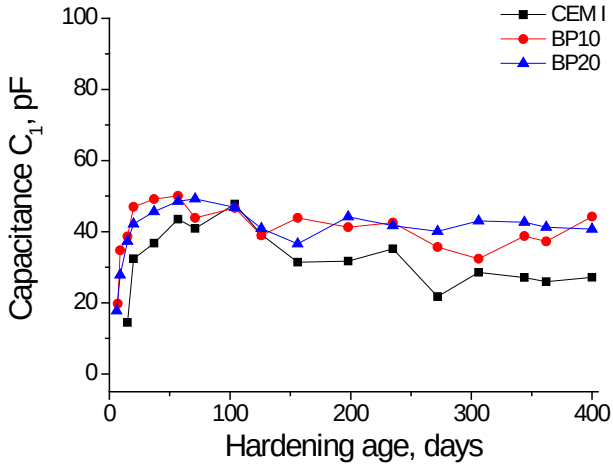

Figure 12. Results of impedance spectroscopy capacitance C_1 for the studied mortars.

The results of capacitance C_2 are depicted in Figure 13Figure 13. This capacitance increased up to 100 days approximately, and from then to 400 days it kept almost constant or hardly decreased, depending on the kind of mortars. The values of capacitance C_2 were higher for mortars with brick powder, especially for BP20 ones, compared to those prepared with CEM I without addition.

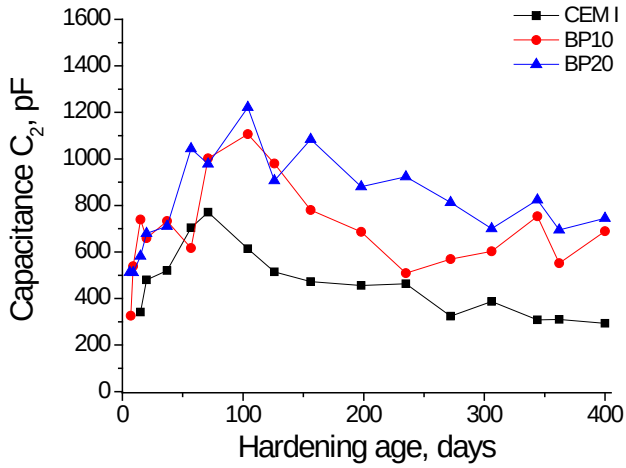

Figure 13. Results of impedance spectroscopy capacitance C_2 for the studied mortars.

3.3. Differential ThermalThermogrvimetric Analysisanalysis

Con formato: Fuente: Cursiva
Con formato: Fuente: Cursiva
Con formato: Fuente: Cursiva
Con formato: Fuente: Cursiva
Con formato: Fuente: Cursiva
Con formato: Inglés (Reino Unido)
Con formato: Fuente: Cursiva
Con formato: Fuente: Cursiva
Con formato: Fuente: Cursiva
Con formato: Fuente: Cursiva
Con formato: Fuente: Cursiva
Con formato: Fuente: Cursiva

The derivate of weight versus temperature curves obtained for the studied mortars at 15 and 90 hardening ages are shown in Figure 14Figure 14. As can be observed, the area of portlandite peak of those curves was lower for mortars with brick powder, especially for BP20 ones. Table 2 shows the evolution of the percentagearea of the portlandite peak in the sample with age as a function of the content in brick powder. It has been presented as percentage of the initial mass due to the small differences in mass of the samples used for TG tests.

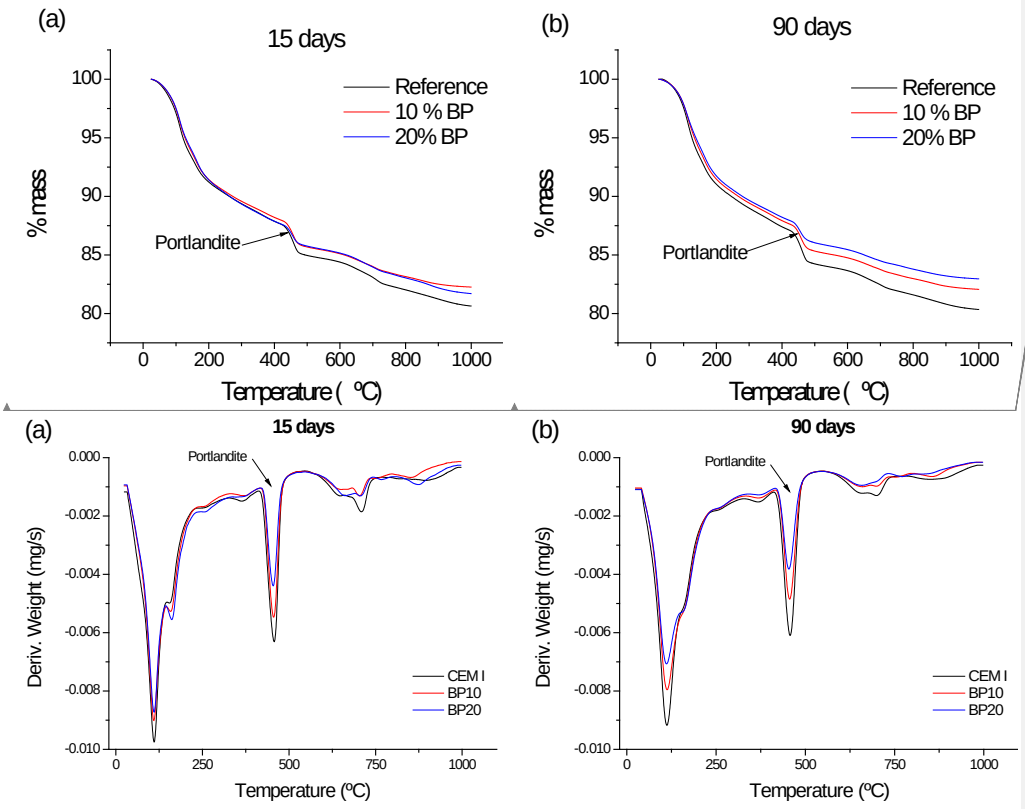

Figure 14. (a) Derivate of weight versusPercentage of mass vs temperature (TG) curve obtained for the studied mortars at 15 hardening days. (b) Percentage of mass vs temperature (TG) curve Derivate of weight versus temperature curve obtained for the analysed mortars at 90 hardening days.

Table 2. Area of the portlandite peakPercentage of porlandite in the sample as a function of age and binder used

Binder designation	15 days	90 days	% increase
CEM I	11.43%0.2844	12.16%0.3081	6.378.33

Con formato: Inglés (Reino Unido)

Código de campo cambiado

Código de campo cambiado

Tabla con formato

BP10	9.09%0.1525	9.24%0.1458	1.61-4.37
BP20	7.62%0.1110	7.57%0.1081	-0.58-2.65

337

338 *3.4. Capillary absorption test*

339 The parameters obtained from this test, as has been previously explained, are the capillary
340 suction coefficient *K* and the effective porosity of the samples. The results of the capillary suction
341 coefficient *K* are depicted in Figure 15Figure 15. For CEM I mortars, this coefficient hardly changed
342 along the studied period. On the other hand, for mortars with brick powder the coefficient K
343 decreased with time, although for BP10 ones this decrease was continuously produced between 28
344 and 400 days, while for BP20 mortars it was mainly noted from 28 to 200 days. At 400 days, the
345 coefficient *K* values were similar for both kinds of brick powder specimens and lower than those
346 observed for CEM I ones.

Con formato: Fuente: Cursiva

Con formato: Fuente: Cursiva

Con formato: Inglés (Reino Unido)

Con formato: Fuente: Cursiva

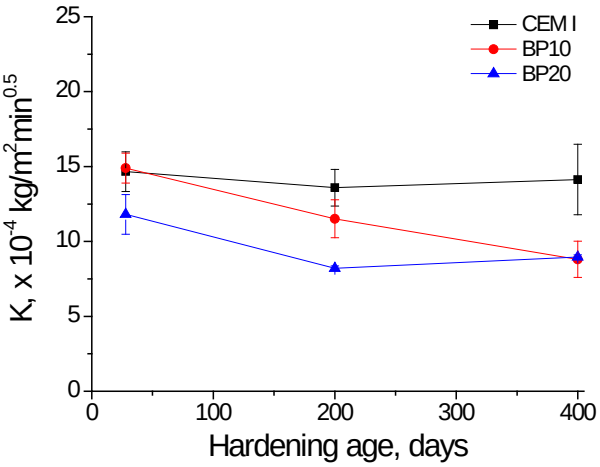

347
348 **Figure 15.** Results of capillary suction coefficient (K) for CEM I, BP10 and BP20 mortar samples.
349

350 The effective porosity results can be observed in Figure 16Figure 16. This porosity scarcely
351 decreased with hardening age for the analysed mortars. Along the studied period, the lowest
352 effective porosity values always corresponded to BP20 mortars, whereas the highest ones were
353 noted for CEM I specimens.

Con formato: Inglés (Reino Unido)

354

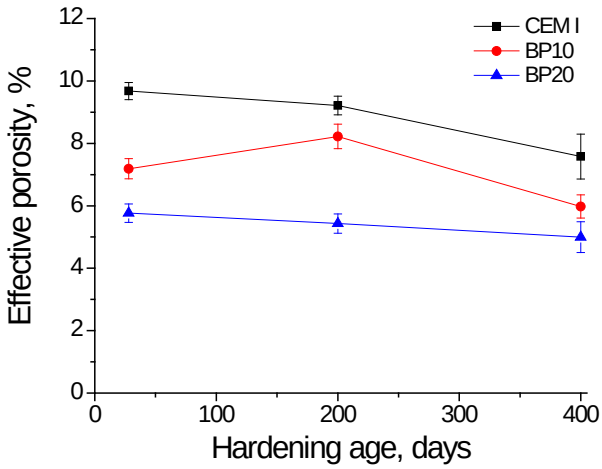

Figure 16. Results of effective porosity for the studied mortars.

3.5. Steady-state diffusion coefficient obtained from saturated sample's resistivity

The changes with time of the steady-state chloride diffusion coefficient obtained from saturated sample's resistivity are shown in Figure 17Figure 17. This parameter hardly rose with hardening age for CEM I mortars, while it slightly decreased for BP10 and BP20 ones. Throughout this research, the mortars with brick powder showed lower diffusion coefficient values compared to CEM I ones.

Con formato: Inglés (Reino Unido)

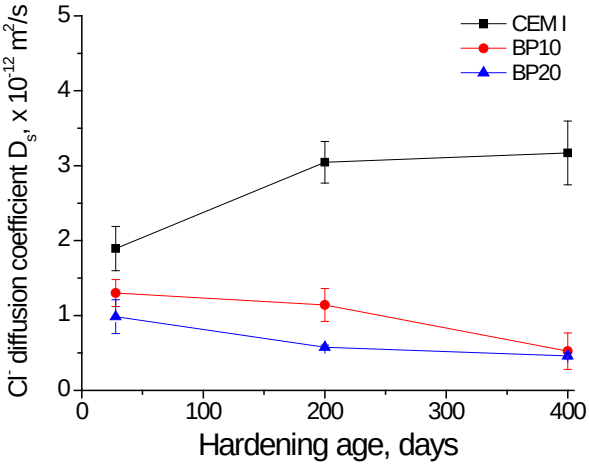

Figure 17. Results of the steady-state chloride diffusion coefficient obtained from the resistivity of saturated samples of CEM I, BP10 and BP20 mortars.

367

368 *3.6. Forced migration test*

369 The results of the non-steady-state chloride migration coefficient D_{NTB} obtained for the studied
370 mortars are depicted in Figure 18Figure 18. This parameter scarcely decreased with hardening time
371 for all the specimens including brick powder, but it increased for samples prepared with OPC. The
372 values of chloride migration coefficient were very similar for mortars with brick powder and they
373 were considerably lower than those noted for CEM I ones.

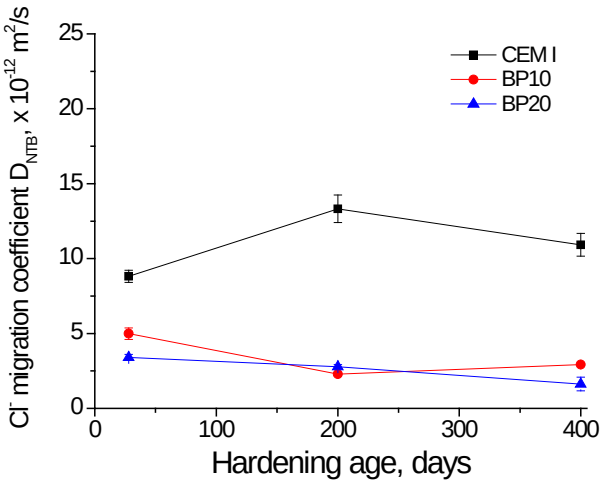

374
375 **Figure 18.** Results of the non-steady-state chloride migration coefficient for CEM I, BP10 and BP20
376 mortars.

377

378 *3.7. Mechanical strength test*

379 The results of compressive and flexural strengths obtained for the studied mortars are depicted
380 in Figure 19Figure 19 and Figure 20Figure 20 respectively. The compressive strength rose with
381 hardening age for all the studied mortars, although the increasing rate of this parameter was
382 scarcely higher for CEM I and BP10 specimens. Despite that, at 400 days there were hardly
383 compressive strength differences among the different kinds of mortars. On the other hand, the
384 flexural strength kept practically constant over the 400-days period, and it was slightly greater for
385 mortars with brick powder in comparison with CEM I ones.

Con formato: Inglés (Reino Unido)

Con formato: Inglés (Reino Unido)

Con formato: Inglés (Reino Unido)

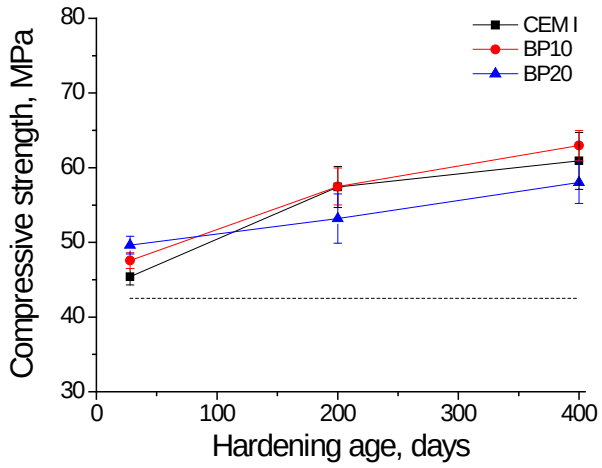

Figure 19. Results of compressive strength for the studied mortars.

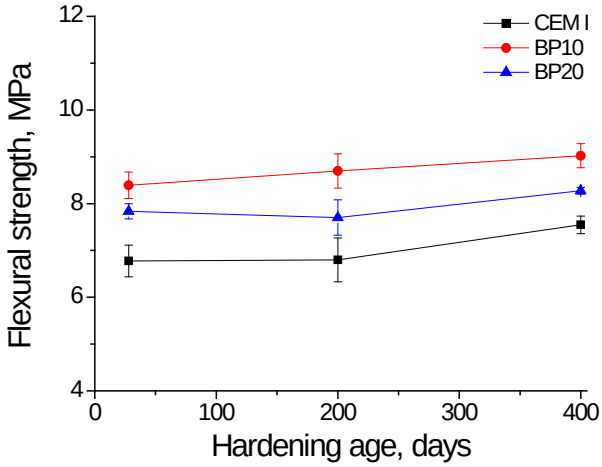

Figure 20. Results of flexural strength for the studied mortars.

4. Discussion

4.1. Microstructure characterisation

Regarding the mercury intrusion porosimetry results, the general decrease of the total porosity observed in the short-term (see Figure 7Figure 7) could be related to the progressive development of clinker hydration [49,50][28] and the pozzolanic reactions of brick powder [9,11], which would form new solid phases, reducing the volume of pores of the materials. The similar values of total porosity obtained for CEM I and BP10 mortars would mean that a replacement of a 10% of clinker by brick

Con formato: Inglés (Reino Unido)

powder would hardly have an influence on this parameter. On the other hand, the highest values of total porosity noted up to 200 days for BP20 specimens could be explained in relation to their higher volume of brick powder addition. The development of pozzolanic reactions of brick powder would need the presence of portlandite produced by clinker hydration [11]. The content of clinker for BP20 mortars was lower than for BP10 ones, therefore at the same hardening ages, it is expected that less amount of portandite has been formed for BP20 specimens. This lower availability of portlandite would could produce a slight delay in the development of brick powder pozzolanic reactions for BP20 mortars [15], entailing that more time was needed in order to reduce total porosity. The increase of the total porosity between 200 and 400 days could be due to shrinkage since this increase is lower for BP20 samples. This result suggests that in addition to certain pozzolanic activity, they may act as filler, as could be expected since they present some quartz (see Figure 1Figure 1). The reaction promotes pore network refinement, leading to greater shrinkage [48], but the filler acts as a reducer of that phenomenon [49]. The BP20 has more addition, and as a consequence more filler and that could be the reason of the smaller increase in porosity.

Con formato: Inglés (Reino Unido)

With respect to the pore size distributions of the studied mortars (see Figure 8Figure 8), the greater pore refinement observed as the content of brick powder was higher, could be due to the development of pozzolanic reactions of this addition [9,11]. As products of these reactions, additional CSH phases would be formed [12], reducing the pore sizes. Furthermore, the microstructure refinement with hardening time noted for the studied mortars, especially for BP10 and BP20 ones, could be again a result of the progressive development of hydration and pozzolanic reactions [16]. This development would be more time extended for those pozzolanic ones, as suggested the pore size distribution results for brick powder mortars at 200 and 400 days. The Hg retained results (see Figure 9Figure 9) overall coincided with pore size distributions previously discussed. The higher values of this parameter observed for brick powder mortars would show a greater tortuosity of their pore network, which would be in keeping with their higher refinement.

Con formato: Inglés (Reino Unido)

Con formato: Inglés (Reino Unido)

The pozzolanic activity of the addition can be confirmed by the TG-DTA results (see Figure 14 and Table 2). For CEM I the amount of portlandite increased from 15 to 90 days due to the progress of the hydration reactions of the clinker. For BP10 and BP20 samples the amount of portlandite decreaseddid not increase much, or even decreased, due to the consumption of portlandite in the pozzolanic reactions. This effect is more important in BP10, confirming the hypothesis of the slowing down of the pozzolanic reactions in the BP20 because of the lower amount of portlandite available, as suggested before. These results are in agreement with previously published papers [11,16].

In relation to impedance spectroscopy results, both resistances R_1 and R_2 are related to the electrolyte which fills the pores of the sample [40]. However, the resistance R_1 is associated only with the percolating pores of the sample [40], while resistance R_2 provides information about all the pores of the sample (both occluded and percolating ones) [40]. The increase with age of both resistances and the higher values showed by brick powder mortars (see Figure 10Figure 10 and Figure 11Figure 11) would agree with mercury intrusion porosimetry results, mainly with their important pore refinement, which was explained in relation to the development of hydration and pozzolanic reactions [12]. The greater resistances R_2 noted for BP20 mortars could also have relation with the higher microstructure refinement of those mortars, particularly at 200 and 400 days. In addition to this, the higher values of the resistances from the initial stage would confirm the filler effect of the addition. The porosity of the samples is higher for those containing brick powder, while the electrical resistance shows the opposite effect. This result confirms the filler effect [12], because the addition particles could block the currentrefine the whole pore network., but not causing a change in the porosity, as has been schematically represented in Figure 21.

Con formato: Fuente: Cursiva
Con formato: Fuente: Cursiva
Con formato: Fuente: Cursiva
Con formato: Fuente: Cursiva
Con formato: Fuente: Cursiva
Con formato: Fuente: Cursiva
Con formato: Inglés (Reino Unido)
Con formato: Inglés (Reino Unido)
Con formato: Fuente: Cursiva
Con formato: Fuente: Cursiva

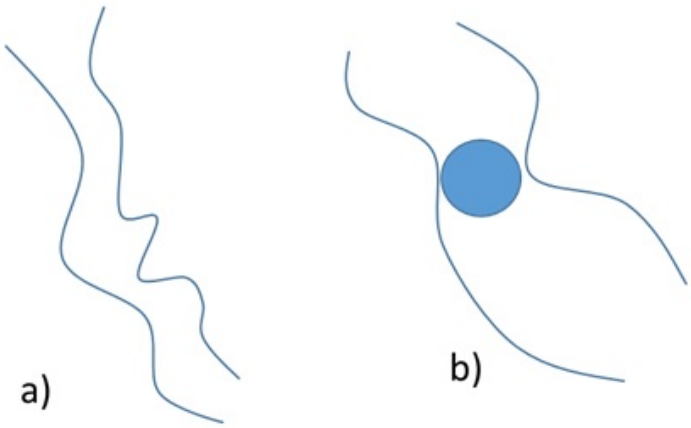

Figure 21. (a) Schematic representation of pore of the microstructure of material. (b) Block of the pore due to the filler effect of the brick powder particles.

The impedance capacitance C_1 is related to the solid fraction of the sample [40]. The values of this parameter hardly differ for the different studied mortars (see Figure 12Figure 12). This would mean that all of them would have a similar solid fraction, independently of their pore size distribution. Therefore, only small porosity differences among them could be expected, which would be in keeping with total porosity results (see Figure 7Figure 7). The rise with time of capacitance C_1, especially in the short-term, would agree with the reduction of total porosity noted from 28 to 100 days. This would be produced by the solid phases formation as products of hydration and pozzolanic reactions [11], as has been already explained. The higher value of C_1 for samples with brick powder reflects the different nature of the solids present in the material, due to the waste.

The capacitance C_2 is associated to the pore surface in contact with the electrolyte which fills the pore network of the material [37]. The rise of this capacitance in the short-term for all the studied mortars would mean that the pore surface increased, likely due to rough structures formed by the new solids made as products of clinker hydration [28] and brick powder pozzolanic reactions [11]. The higher capacitance C_2 values noted for mortars which incorporate brick powder would be in accordance with their more refined microstructure showed by mercury intrusion porosimetry.

Con formato: Justificado, Interlineado: Doble

Con formato: Sangría: Primera línea: 0,75 cm, Sin viñetas ni numeración

Con formato: Fuente: Cursiva

Con formato: Fuente: Cursiva

Con formato: Inglés (Reino Unido)

Con formato: Inglés (Reino Unido)

Con formato: Fuente: Cursiva

Con formato: Fuente: Cursiva

Con formato: Fuente: Cursiva

Con formato: Fuente: Cursiva

Con formato: Fuente: Cursiva

Con formato: Fuente: Cursiva

Con formato: Fuente: Cursiva

Con formato: Fuente: Cursiva

However, in the long-term this capacitance did not rise, or even slightly decreased, which was more noticeable for brick powder samples. This result could be explained in relation to the progressive silting of the pores, as a consequence of the prolonged development of hydration and pozzolanic reactions [12], which would produce a progressive pores filling and closing of the microstructure [27].

Lastly, considering the study of the microstructure of the analysed mortars, all of them agree in that the addition of 10% and 20% of waste brick powder entailed an improvement of pore structure of the mortars in both short- and long-term.

4.2. Durability-related parameters

The importance of the capillary suction coefficient K and effective porosity has been widely reported [51][44]. The results of both parameters (see Figure 15Figure 15 and Figure 16Figure 16) were overall in keeping with those obtained in the characterisation of microstructure. The lowest coefficient K and effective porosity values observed for brick powder mortars would indicate a higher difficulty of water ingress in those mortars in comparison with CEM I ones, even though the total porosity was always higher. This result confirms that both the pozzolanic activity and the filler effect of the addition are positive from the point of view of the durability, because the combination of both effects causes a more refined pore network [12,49].

The analysis of the influence of brick powder addition with respect to chloride ingress resistance of the materials is interesting, because this aggressive ion is one of the most common causes of the corrosion of reinforcing elements. Here, the resistance against chloride ingress was studied through the steady-state diffusion coefficient (D_s), obtained from saturated sample's resistivity, and with the non-steady-state migration coefficient (D_{NTB}). Both coefficients were lower for brick powder mortars along the studied time period (see Figure 17Figure 17 and Figure 18Figure 18). Again, this could be due to the higher pore network refinement of BP10 and BP20 mortars

Con formato: Fuente: Cursiva

Con formato: Inglés (Reino Unido)

Con formato: Inglés (Reino Unido)

Con formato: Fuente: Cursiva

Con formato: Fuente: Cursiva

Con formato: Fuente: Cursiva

Con formato: Fuente: Cursiva

Con formato: Inglés (Reino Unido)

Con formato: Inglés (Reino Unido)

compared to CEM I, as revealed the mercury intrusion porosimetry and impedance spectroscopy techniques, whose results were previously discussed.

Finally, according to the analysis of the previously discussed parameters, all of them would indicate that the replacement of 10% and 20% of clinker by waste brick powder would improve the durability properties of the mortars throughout the 400-days studied period.

4.3. Mechanical strength results

The study of the performance of cement-based materials related to their mechanical strength is important, because the strength constitutes one of the most important requirements of concrete and other cement-based materials structural elements. In this work, both compressive and flexural strengths were studied. Both parameters were similar or even higher for brick powder mortars in comparison with CEM I specimens (see Figure 19Figure 19 and Figure 20Figure 20). This result would be in accordance with those obtained in the microstructure characterisation and for the durability-related parameters, already described and discussed. They would show the beneficial effect of the addition of brick powder in the performance of cement mortars [12]. It is important to notice that all the materials fulfil the requirement of the standard about the compressive strength of mortars. This requirement is included in Figure 19Figure 19 with a dotted line.

Con formato: Inglés (Reino Unido)

Con formato: Inglés (Reino Unido)

Con formato: Inglés (Reino Unido)

5. Conclusions

The main conclusions that can be drawn from the results previously discussed can be summarized as follows:

- The microstructure characterisation performed in this research would confirm the pozzolanic activity of the waste brick powder. The effect of this pozzolanic activity was more noticeable for mortars with 10% of brick powder, because of the higher amount of portlandite available compared to those with 20% of this addition.

- The waste brick powder would also act as filler, reducing the effect of the greater shrinkage phenomenon, which is likely produced by the higher pore refinement due to the development of the pozzolanic reactions of this addition.
- The pore structure of all the studied mortars became more refined with hardening age, probably due to the progressive development of clinker hydration and pozzolanic reactions of brick powder.
- Mortars with waste brick powder showed higher microstructure refinement compared to CEM I ones, which could be related to combined action of the additional solid phases formed as products of pozzolanic reactions of brick powder and the filler effect of this addition.
- The results of the non-destructive impedance spectroscopy technique are overall in keeping with those obtained with mercury intrusion porosimetry. Therefore, the impedance spectroscopy can be used for following the pore network development of mortars which incorporate waste brick powder as clinker replacement. Moreover, the impedance resistances results would confirm the filler effect of this addition.
- The addition of waste brick powder up to 20% of the binder, would entail an improvement of the durability-related properties of the mortars, especially their chloride ingress resistance, compared to CEM I mortars. This positive performance could be due to their more refined pore network produced by both the pozzolanic activity and the filler effect of this addition.
- The addition of 10% and 20% of waste brick powder did not produce a loss of compressive strength of the mortars, which fulfilled the compressive strength values required by the corresponding standard.
- According to the results obtained in this research, mortars which incorporated 10% and 20% of waste brick powder as clinker replacement, showed good service properties in the

long-term (400 days), even better than those made with ordinary Portland cement without additions.

6. Acknowledgments

The research work included in the paper has been financially supported by project DFP17-0006 "Aplicación de un tratamiento térmico para mejorar las prestaciones mecánicas de residuos de mampostería como reemplazo de cemento", funded by Universidad de La Frontera (Chile). The authors also wish to thank Cementos Portland Valderrivas S.A. for providing the ordinary Portland cement used in this study.

Declarations of interest: none

7. References

[1] M.J. Shannag, A. Yeginobali, Properties of pastes, mortars and concretes containing natural pozzolan, Cem. Concr. Res. 25 (1995) 647–657. doi:10.1016/0008-8846(95)00053-F.

[2] M. Nili, A.M. Salehi, Assessing the effectiveness of pozzolans in massive high-strength concrete, Constr. Build. Mater. 24 (2010) 2108–2116. doi:10.1016/J.CONBUILDMAT.2010.04.049.

[3] M. Glinicki, D. Jóźwiak-Niedźwiedzka, K. Gibas, M. Dąbrowski, Influence of Blended Cements with Calcareous Fly Ash on Chloride Ion Migration and Carbonation Resistance of Concrete for Durable Structures, Materials (Basel). 9 (2016) 18. doi:10.3390/ma9010018.

[4] J. Bijen, Benefits of slag and fly ash, Constr. Build. Mater. 10 (1996) 309–314. doi:10.1016/0950-0618(95)00014-3.

[5] J. Payá, J. Monzó, M. V. Borrachero, F. Amahjour, I. Girbés, S. Velázquez, et al., Advantages in the use of fly ashes in cements containing pozzolanic combustion residues: Silica fume, sewage sludge ash, spent

565 fluidized bed catalyst and rice husk ash, J. Chem. Technol. Biotechnol. 77 (2002) 331–335.
566 doi:10.1002/jctb.583.
567 [6] A. Bouikni, R.N. Swamy, A. Bali, Durability properties of concrete containing 50% and 65% slag,
568 Constr. Build. Mater. 23 (2009) 2836–2845. doi:10.1016/j.conbuildmat.2009.02.040.
569 [7] W. Xu, Y.T. Lo, W. Wang, D. Ouyang, P. Wang, F. Xing, Pozzolanic Reactivity of Silica Fume and
570 Ground Rice Husk Ash as Reactive Silica in a Cementitious System: A Comparative Study, Mater. . 9
571 (2016). doi:10.3390/ma9030146.
572 [8] Y.-H. Kwon, S.-H. Kang, S.-G. Hong, J. Moon, Intensified Pozzolanic Reaction on Kaolinite Clay-Based
573 Mortar, Appl. Sci. . 7 (2017). doi:10.3390/app7050522.
574 [9] L.A. Pereira-De-Oliveira, J.P. Castro-Gomes, P.M.S. Santos, The potential pozzolanic activity of glass
575 and red-clay ceramic waste as cement mortars components, Constr. Build. Mater. 31 (2012) 197–203.
576 doi:10.1016/j.conbuildmat.2011.12.110.
577 [10] J. Katzer, Strength performance comparison of mortars made with waste fine aggregate and ceramic
578 fume, Constr. Build. Mater. 47 (2013) 1–6. doi:10.1016/j.conbuildmat.2013.04.039.
579 [11] E. Navrátilová, P. Rovnaníková, Pozzolanic properties of brick powders and their effect on the
580 properties of modified lime mortars, Constr. Build. Mater. 120 (2016) 530–539.
581 doi:10.1016/j.conbuildmat.2016.05.062.
582 [12] A. Schackow, D. Stringari, L. Senff, S.L. Correia, A.M. Segadães, Influence of fired clay brick waste
583 additions on the durability of mortars, Cem. Concr. Compos. 62 (2015) 82–89.
584 doi:10.1016/j.cemconcomp.2015.04.019.
585 [13] H. Böke, S. Akkurt, B. Ipekoğlu, E. Uğurlu, Characteristics of brick used as aggregate in historic
586 brick-lime mortars and plasters, Cem. Concr. Res. 36 (2006) 1115–1122.

587 doi:10.1016/j.cemconres.2006.03.011.

588 [14] F. Puertas, A. Barba, M.F. Gazulla, M.P. Gómez, M. Palacios, S. Martínez-ramírez, Ceramic wastes as
589 raw materials in portland cement clinker fabrication: Characterization and alkaline activation , Mater.
590 Constr. 56 (2006) 73–84.

591 [15] A. Naceri, M.C. Hamina, Use of waste brick as a partial replacement of cement in mortar, Waste Manag.
592 29 (2009) 2378–2384. doi:10.1016/j.wasman.2009.03.026.

593 [16] T. Vieira, A. Alves, J. de Brito, J.R. Correia, R. V. Silva, Durability-related performance of concrete
594 containing fine recycled aggregates from crushed bricks and sanitary ware, Mater. Des. 90 (2016) 767–
595 776. doi:10.1016/j.matdes.2015.11.023.

596 [17] A.A. Aliabdo, A.-E.M. Abd-Elmoaty, H.H. Hassan, Utilization of crushed clay brick in concrete
597 industry, Alexandria Eng. J. 53 (2014) 151–168. doi:10.1016/j.aej.2013.12.003.

598 [18] T. Kulovaná, E. Vejmelková, M. Keppert, P. Rovnaníková, Z. Keršner, R. Černý, Mechanical, durability
599 and hygrothermal properties of concrete produced using Portland cement-ceramic powder blends,
600 Struct. Concr. 17 (2016) 105–115. doi:10.1002/suco.201500029.

601 [19] A.E. Lavat, M.A. Trezza, M. Poggi, Characterization of ceramic roof tile wastes as pozzolanic
602 admixture, Waste Manag. 29 (2009) 1666–1674. doi:10.1016/j.wasman.2008.10.019.

603 [20] Z. Ge, Z. Gao, R. Sun, L. Zheng, Mix design of concrete with recycled clay-brick-powder using the
604 orthogonal design method, Constr. Build. Mater. 31 (2012) 289–293.
605 doi:10.1016/j.conbuildmat.2012.01.002.

606 [21] Z. Ge, Y. Wang, R. Sun, X. Wu, Y. Guan, Influence of ground waste clay brick on properties of fresh and
607 hardened concrete, Constr. Build. Mater. 98 (2015) 128–136. doi:10.1016/j.conbuildmat.2015.08.100.

608 [22] L. Zheng, Z. Ge, Z. Yao, Z. Gao, Mechanical properties of mortars with recycled clay-brick-powder, in:

609 Proc. 11th Int. Conf. Chinese Transp. Prof. ICCTP 2011, American Society of Civil Engineers, Nanjing,
610 China, n.d.: pp. 3379–3388.
611 [23] V. Baroghel-Bouny, Water vapour sorption experiments on hardened cementitious materials, Cem.
612 Concr. Res. 37 (2007) 414–437. doi:10.1016/j.cemconres.2006.11.019.
613 [24] Q. Wang, P. Yan, J. Yang, B. Zhang, Influence of steel slag on mechanical properties and durability of
614 concrete, Constr. Build. Mater. 47 (2013) 1414–1420. doi:10.1016/j.conbuildmat.2013.06.044.
615 [25] J. Payá, V. Borrachero, E. Peris-Mora, A. Aliaga, J. Monzó, Improvement of Portland cement/fly ash
616 mortars strength using classified fly ashes, in: Stud. Environ. Sci., 1994: pp. 563–570.
617 doi:10.1016/S0166-1116(08)71489-4.
618 [26] K.O. Ampadu, K. Torii, M. Kawamura, Beneficial effect of fly ash on chloride diffusivity of hardened
619 cement paste, Cem. Concr. Res. 29 (1999) 585–590. doi:10.1016/S0008-8846(99)00047-2.
620 [27] J.M. Ortega, M.D. Esteban, R.R. Rodríguez, J.L. Pastor, I. Sánchez, Microstructural Effects of Sulphate
621 Attack in Sustainable Grouts for Micropiles, Materials (Basel). 9 (2016). doi:10.3390/ma9110905.
622 [28] J.M. Ortega, I. Sánchez, M.A. Climent, Impedance spectroscopy study of the effect of environmental
623 conditions in the microstructure development of OPC and slag cement mortars, Arch. Civ. Mech. Eng.
624 15 (2015) 569–583. doi:10.1016/j.acme.2014.06.002.
625 [29] S. Xu, J. Wang, Q. Jiang, S. Zhang, Study of natural hydraulic lime-based mortars prepared with
626 masonry waste powder as aggregate and diatomite/fly ash as mineral admixtures, J. Clean. Prod. 119
627 (2015) 118–127. doi:10.1016/j.jclepro.2016.01.069.
628 [30] H. Li, L. Dong, Z. Jiang, X. Yang, Z. Yang, Study on utilization of red brick waste powder in the
629 production of cement-based red decorative plaster for walls, J. Clean. Prod. 133 (2016) 1017–1026.
630 doi:10.1016/j.jclepro.2016.05.149.

631 [31] ASTM, ASTM C204-16 Standard Test Methods for Fineness of Hydraulic Cement by Air Permeability
632 Apparatus, (2016) 10.
633 [32] AENOR, UNE-EN 197-1:2011. Composición, especificaciones y criterios de conformidad de los
634 cementos comunes., (2000) 30.
635 http://www.aenor.es/aenor/normas/normas/fichanorma.asp?tipo=N&codigo=N0048623&PDF=Si#.VkT
636 Sx_kvcdU (accessed November 12, 2015).
637 [33] AENOR, UNE-EN 196-1:2005. Métodos de ensayo de cementos. Parte 1: Determinación de resistencias
638 mecánicas, (2005).
639 http://www.aenor.es/aenor/normas/normas/fichanorma.asp?tipo=N&codigo=N0034791&PDF=Si#.Vld
640 HF_kvcdU (accessed November 26, 2015).
641 [34] S. Diamond, Aspects of concrete porosity revisited, Cem. Concr. Res. 29 (1999) 1181–1188.
642 doi:10.1016/S0008-8846(99)00122-2.
643 [35] S. Diamond, Mercury porosimetry, Cem. Concr. Res. 30 (2000) 1517–1525.
644 doi:10.1016/S0008-8846(00)00370-7.
645 [36] M. Cabeza, P. Merino, A. Miranda, X.R. Nóvoa, I. Sanchez, Impedance spectroscopy study of hardened
646 Portland cement paste, Cem. Concr. Res. 32 (2002) 881–891. doi:10.1016/S0008-8846(02)00720-2.
647 [37] M. Cabeza, M. Keddam, X.R. Nóvoa, I. Sánchez, H. Takenouti, Impedance spectroscopy to characterize
648 the pore structure during the hardening process of Portland cement paste, Electrochim. Acta. 51 (2006)
649 1831–1841. doi:10.1016/j.electacta.2005.02.125.
650 [38] J.M. Cruz, I.C. Fita, L. Soriano, J. Payá, M.V. Borrachero, The use of electrical impedance spectroscopy
651 for monitoring the hydration products of Portland cement mortars with high percentage of pozzolans,
652 Cem. Concr. Res. 50 (2013) 51–61. doi:10.1016/j.cemconres.2013.03.019.

653 [39] B. Díaz, X.R. Nóvoa, M.C. Pérez, Study of the chloride diffusion in mortar: A new method of
654 determining diffusion coefficients based on impedance measurements, Cem. Concr. Compos. 28 (2006)
655 237–245. doi:10.1016/j.cemconcomp.2006.01.009.
656 [40] M. Cabeza, P. Merino, A. Miranda, X.R. Nóvoa, I. Sanchez, Impedance spectroscopy study of hardened
657 Portland cement paste, Cem. Concr. Res. 32 (2002) 881–891. doi:10.1016/S0008-8846(02)00720-2.
658 [41] E. Barsoukov, J.R. Macdonald, Impedance Spectroscopy, John Wiley & Sons, Inc., Hoboken, NJ, USA,
659 2005. doi:10.1002/0471716243.
660 [42] Z. Vladikova, D; Zoltowski, P., Makowska, E., Stoynov, Selectivity study of the differential impedance
661 analysis—comparison with the complex non-linear least-squares method, Electrochim. Acta. 47 (2002)
662 2943–2951. doi:10.1016/S0013-4686(02)00187-1.
663 [43] AENOR, UNE 83982:2008. Durabilidad del hormigón. Métodos de ensayo. Determinación de la
664 absorción de agua por capilaridad del hormigón endurecido. Método Fagerlund., (2008).
665 http://www.aenor.es/aenor/normas/normas/fichanorma.asp?tipo=N&codigo=N0041389#.VpPtyxXhAd
666 U (accessed January 11, 2016).
667 [44] J.M. Ortega, I. Sanchez, C. Anton, G. de Vera, M.A. Climent, Influence of Environment on Durability of
668 Fly Ash Cement Mortars, ACI Mater. JournalMaterials J. 109 (2012) 647–656.
669 https://www.concrete.org/publications/internationalconcreteabstractsportal.aspx?m=details&ID=51684
670 162 (accessed October 25, 2015).
671 [45] Rilem recommendation TC 116-PCD. Permeability of concrete as a criterion of its durability., Mater.
672 Struct. 32 (1999) 174–179.
673 [46] C. Andrade, C. Alonso, A. Arteaga, P. Tanner, Methodology based on the electrical resistivity for the
674 calculation of reinforcement service life, in: V.M. Malhotra (Ed.), Proc. 5th CANMET/ACO Int. Conf.

675 Durab. Concr. Suppl. Pap., American Concrete Institute, Barcelona, Spain, 2000: pp. 899–915.

676 [47] Nordtest., NT Build 492. Concrete, mortar and cement-based repair materials: chloride migration

677 coefficient from non-steady-state migration experiments., (1999) 8.

678 [48] K. Kovler, S. Zhutovsky, Overview and future trends of shrinkage research, Mater. Struct. Constr. 39

679 (2006) 827–847. doi:10.1617/s11527-006-9114-z.

680 [49] M. Singh, A. Srivastava, D. Bhunia, An investigation on effect of partial replacement of cement by waste

681 marble slurry, Constr. Build. Mater. 134 (2017) 471–488. doi:10.1016/j.conbuildmat.2016.12.155.

682